Effects of Cu on the microstructural and mechanical properties of sputter deposited Ni-Ti thin films

M. Callisti [a], F. D. Tichelaar [b], B. G. Mellor [c], T. Polcar [a,d]

[a] National Centre for Advanced Tribology at Southampton, Faculty of Engineering and the Environment, University of Southampton, Southampton SO17 1BJ, UK

[b] Delft University of Technology, Kavli Institute of Nanoscience, National Center for HREM, Lorentzweg 1, 2628CJ, Delft, The Netherlands

[c] Materials Research Group, Faculty of Engineering and the Environment, University of Southampton, Southampton SO17 1BJ, UK

[d] Department of Control Engineering, Faculty of Electrical Engineering, Czech Technical University in Prague, Technická 2, Prague 6, Czech Republic

Corresponding author:

Mauro Callisti

mc3a09@soton.ac.uk

National Centre for Advanced Tribology at Southampton - Highfield Campus

Building 5 (Eustice)/ Room 3025 – Mailpoint M7

Southampton, Hampshire SO171BJ

United Kingdom

Tel.: +44 (0)23 8059 2351

Abstract

The microstructure of sputter deposited Ti-rich Ni-Ti thin films doped with Cu in the range 0-20.4 at.% and annealed for 1 h at 500 and 600°C has been investigated and correlated with the mechanical properties of the films measured by depth-sensing nanoindentation. X-ray diffraction analysis showed the microstructural evolution of Ni-Ti thin films when doped with Cu and annealed at different temperatures. Heat treatments promoted the nucleation and growth of Ti_2Ni precipitates in Ti-rich Ni-Ti thin films, which affected the stability of austenitic and martensitic phases at ambient temperature. Doping with Cu caused the formation of $Ti(Ni, Cu)_2$ plate precipitates, which became more finely and densely dispersed in the grains with increasing Cu content. TEM analysis showed a columnar grain morphology extended through the whole films thickness, while with increasing Cu content a noticeable lateral grain refinement was induced by segregation of a (Ni, Cu)-rich phase to grain boundaries. The nano-hardness increased almost linearly with increasing Cu content owing to this grain refinement, though differences between samples annealed at different temperatures were found which could be related to the evolution of $Ti(Ni, Cu)_2$ plate precipitates with annealing temperature and Cu content. The Young's modulus exhibited a similar dependence on Cu content as nano-hardness, though no significant differences were observed with increasing annealing temperatures.

Keywords: Shape memory alloys, Thin films, Sputtering, Nanoindentation, Grain boundary segregation, Precipitation, Grain size.

Introduction

Ni-Ti shape memory alloys are known to exhibit unusual mechanical and functional properties even at the micro- and nano-scale when they are produced in the form of thin films

by PVD techniques [1]. Many studies have thus investigated the behaviour of sputter deposited Ni-Ti thin films for their prospective use in micro-electro-mechanical systems (MEMS) owing to their ability to recover a large transformation stress and strain during thermal cycling, as well as possessing a high actuation rate and work output-to-volume ratio compared to other types of actuators [2]. However, considerably fewer studies have investigated the potential use of such smart thin films as protective or functional layers for tribological applications [3-5].

Although considerable breakthroughs have been achieved by means of extensive research, there are still some concerns regarding the use of these films in industrial applications on account of the inability to control precisely their response to external stimuli. Moreover, in addition to this limitation, low hardness and wear resistance further limit their field of application. To counter these deficiencies much effort has been directed to making Ni-Ti thin films more attractive and the use of a third element as dopant has emerged as an effective approach for changing or modulating their properties [6, 7].

Among the possible candidate dopants elements, Cu is one of the most promising as it reduces the compositional sensitivity of the transformation temperatures, reduces the temperature hysteresis, stabilizes the shape memory effect and increases the actuation rate and the recoverable strain, even under a stresses as high as 1 GPa [8-12]. The properties reported above are strictly dependent on the films microstructure and in particular on the grain size, the formation of different types of precipitates as a function of Cu content and the post-deposition heat treatment [13]. The microstructural evolution of relatively thick (7-9 μm) Ti-rich [14, 15] and (Ni, Cu)-rich [16] Ni-Ti-Cu thin films for a wide range of Cu content and annealing temperatures has been studied. Essentially, annealing temperatures close to that of crystallisation cause the formation of fine plate precipitates coherent with the matrix. In Ti-rich compositions, they are considered to be Guinier-Preston (GP) zones with a body centred crystal structure and a coherent interface with the austenitic (B2) matrix. In (Ni, Cu)-rich

compositions, precipitates are still coherent with the matrix and with a plate-like shape but with a C_{11b}-type crystal structure [17]. As this is metastable phase, with increasing annealing temperature these precipitates evolve losing their coherency with the matrix promoting the formation of semi-coherent spherical precipitates for Ti-rich compositions, or still plate-like but semi-coherent precipitates for (Ni, Cu)-rich compositions, as well as grain boundary precipitates. It has been reported that coherent plate precipitates can disturb the movement of twin boundaries, though the growing martensite can pass through such precipitates deforming them elastically. On the other hand, semi-coherent precipitates in the grain disturb or impede the growth of martensite variants, thus decreasing the amount of strain accommodated in a reversible manner [8, 19].

The effects of different annealing temperatures on the mechanical properties have been investigated by analysing the nanoindentation response of both Ni-rich and Ti-rich Ni-Ti-based film compositions. It has been observed that with increasing annealing temperature both hardness and Young's modulus increase [20, 21]. The observed trends have been attributed to the increased resistance to plastic deformation induced by precipitation hardening, as well as to a change of the phase transformation sequence and thus of the transformation strain [22]. Zarnetta et al. [23] investigated the mechanical properties of austenitic and martensitic Ni-Ti-Cu thin films through nanoindentation. Even in this case, off-stoichiometric compositions with a constant Cu content exhibited, both at ambient and high temperatures (~80°C), higher hardness and Young's modulus resulting from precipitation hardening.

The effects of Cu and of the annealing temperature on the functional behaviour of Ni-Ti-(Cu) films have been extensively studied, as well as the mechanical response of these films when changing the Ni/Ti ratio for a constant Cu content. However, no investigations have been performed in order to evaluate the effects of Cu on the mechanical properties of sputter deposited Ni-Ti thin films.

Therefore, as Cu additions can change effectively the microstructure of Ni-Ti thin films, it is of interest, especially for the purpose of using such films as protective layers, to assess their mechanical properties as a function of the microstructure produced with respect to the Cu content and annealing temperature. Therefore in this study a Ti-rich Ni-Ti thin film was doped with different amounts of Cu, and its microstructural and mechanical properties were investigated.

Experimental details

Ni-Ti thin films with increasing Cu content were deposited on (100) Si wafers (450 μm thick) by a Plasma-Assisted Magnetron Sputtering (PAMS) system (Helios, Leybold Optics GmbH, Alzenau, Germany). The dense argon plasma generated by an inductively coupled RF plasma source (fitted in the process chamber door) was used to pre-treat the substrate at the beginning of each process, as well as to remove fast growing structures during the deposition, so as to increase the density as well as to reduce the level of defects in the films structure. The chamber was pumped down to a base pressure of 1 x 10^{-7} mbar and each deposition was carried out at a pressure of 5 x 10^{-4} mbar (35 sccm Ar flow) for approximately 35 minutes. The Ni/Ti power ratio was kept constant while the power for the Cu target was raised linearly to increase the Cu content in the films. The substrate holder was rotated at 180 rpm in order to avoid the formation of multilayer-type structures. So as to produce films with an amorphous structure, depositions were performed without any deliberate heating of the substrate; moreover the balanced configuration of the sputtering system did not promote excessive heating of the substrate.

The chemical composition of the thin films was measured by energy dispersive X-ray spectroscopy (EDX, semi-quantitative analysis) attached to a JEOL JSM 6500F field emission gun scanning electron microscope (FEG-SEM), through which the surface and cross-sectional morphology of the films was also observed.

After sputtering, the as-deposited thin films were isothermally annealed in a high vacuum (8 x 10^{-5} mbar) for 1 h at 500 and 600°C, in order to induce a crystalline structure as well as to promote different microstructures. In order to avoid delamination induced by thermal stresses a heating/cooling rate of 5°C/min was adopted above 400°C while below this temperature samples were allowed to cool down naturally to ambient temperature.

The phases produced by annealing were investigated by grazing incidence X-ray diffraction (GIXRD). The grazing angle was set at 5° with a scan step size of 0.02°over an angle range of 2θ = 30 – 80°. The diffraction data were collected by using an X'Pert-Pro Philips diffractometer (PANalytical, ALMELO, The Netherland) with a Cu-target (λ=1.540598 Å). The tube was set at an accelerating voltage of 40 kV and a current of 30 mA. The XRD spectra were analysed the X'Pert HighScore Plus software together with a ICDD PDF-2 database.

The structure of the annealed samples was characterised by transmission electron microscopy (TEM) using a FEI Tecnai F20ST/STEM scanning transmission electron microscope (STEM) at an accelerating voltage of 200 kV. Cross-sectional thin foils for TEM and STEM (Scanning Transmission Electron Microscopy) observations were prepared by mechanical grinding and polishing followed by further thinning to an electron transparent thickness by a dual ion miller (Gatan PIPS, model 691).

Mechanical properties were measured using depth-sensing nanoindentation (Nano-Test Platform 2, Micro-Materials Ltd., Wrexham, UK). A diamond Berkovich indenter (tip radius < 100 nm) was used to perform multiple-load nanoindentation experiments at ambient temperature (~20°C). Each indent consisted of 12 cycles, starting with a penetration depth (first cycle) of approximately 25 nm and with a depth step of ~25 nm per cycle. A final penetration depth greater than 1/10 of the film thickness was deliberately chosen in order to facilitate the interpretation of such measurements, although the mechanical properties for the thin films were evaluated only for penetration depths within 1/10 of the film thickness. The

experiments were carried out using a loading rate of 0.1 mN/s whereas an unloading rate of 0.05 mN/s was set in order to have a larger number of points which could be fitted accordingly to the procedure outlined by Oliver and Pharr [24, 25]. A partial unloading of 30% relative to the maximum load per cycle was assessed to be sufficient for the application of the procedure referred to above. A holding time of 20 seconds at every maximum load was selected to saturate creep effects before unloading. Thermal drift correction on the load-displacement curves was performed using the mean value of the pre- and post-indentation drift calibration data collected during a holding time of 60 seconds. For each film nano-hardness was determined as the average of the hardness values measured after the size effect was saturated and before the appearance of substrate effects, while Young's moduli were calculated from the averaged reduced Young's moduli determined for indentation depths within 1/10 of the film thickness.

Results and discussion

1. Chemical composition and surface morphology

Eight Ti-rich Ni-Ti thin films with increasing Cu in the range 0 – 20.4 at.% and a thickness of 1.4 μm were produced. Table I reports the chemical compositions measured by EDX on the as-deposited films. It was noted that when the power to the Cu target was increased Ni and Ti content decreased at approximately the same rate, indicating no preferential re-sputtering effect of Ni and Ti atoms on the growing structure. For Cu content higher than 4 at.% the chemical composition of the thin films changed from being Ti-rich to (Ni, Cu)-rich. In view of the chemical affinity of Ti and O, the chemical composition of some of the Ti-rich thin films was also measured by EDX after heat treatments at 500 and 600°C and no oxygen was detected on the surface. However, annealing at different temperatures promoted the formation of precipitates with different structure and chemical composition, thus altering the chemical

composition of the matrix, i.e. the material exhibiting phase transformation, and consequently its microstructure.

As-deposited Ti-rich NiTi thin films exhibited a featureless surface, while after annealing at 500 and 600°C, the NiTi-base films exhibited striations on the surface (Fig. 1). It is know that crystalline NiTi-based thin films exhibit particular surface features resulting from large deformation accommodated by martensitic transformation [2]. However, the nature of these features is not yet clear as their appearance has been associated with both the elastic buckling of a thin TiO_2 layer formed on top of the NiTi-based film [26], and with the formation of step-like shape features associated with martensite nucleation at the free surface in the B2 matrix [27]. TEM observations of the present films revealed a thin oxide layer (~10 nm) on top of the annealed films, therefore the appearance of these striation features may be related to both the phenomena referred to above.

2. Structure

Fig. 2 shows the cross sectional scanning electron micrographs of the as-deposited and annealed NiTi-base thin films. Fig. 2a illustrates featureless and homogeneous cross-section morphology for the as-deposited film, indicating a dense amorphous film. The amorphous film was noted to exhibit relatively ductile fracture behaviour during SEM sample preparation. Films annealed at 500°C (Fig. 2b) and 600°C (Fig. 2c) had a fibrous texture across the whole film thickness suggesting the presence of relatively large columnar grains. However, films annealed at 600°C exhibited a slightly denser packed fibrous structure compared to when annealed at 500°C.

2.1 X-ray diffraction analysis

The effects of annealing on the microstructure of the Ni-Ti-(Cu) thin films were analysed first for the NiTi-base composition. Fig. 3 shows the XRD spectra of the NiTi-base film in the as-

deposited and annealed conditions. The as-deposited film exhibited an amorphous structure resulting from the relatively low deposition temperature (~80°C, measured by the pyrometer installed in the deposition chamber floor). After annealing for 1 h at 500°C the XRD spectra revealed the coexistence of the austenitic (B2) and martensitic (B19') phases at ambient temperature indicating that nucleation of martensite in the austenitic matrix took place during cooling from the annealing temperature. However, the martensitic transformation was incomplete, i.e. ambient temperature was between the martensite start (M_s) and finish (M_f) temperatures. Small peaks related to the metastable Ti_2Ni phase were also identified in the film annealed at 500°C. This phase is thought to have a spherical morphology with a semi-coherent interface with the matrix [28]. On the other hand, the film annealed at 600°C exhibited a fully martensitic structure as revealed by the XRD spectrum (Fig. 3), thus indicating M_f above ambient temperature, which was found also in other studies [29]. It is well known that the transformation temperatures of Ni-Ti alloys are strongly affected by both the chemical composition and by stress according to the Clausius-Clapeyron relationship [30]. In the results reported in Fig. 3 no appreciable shifts in peaks due to residual stresses were noted for the two annealing temperatures, therefore the shift of transformation temperatures is mainly attributable to the change of chemical composition of the matrix. Fig. 3 shows that with increasing annealing temperature the peaks related to the Ti_2Ni phase became more intense, indicating an increasing amount of this phase with concomitant Ni and Ti depletion in the matrix. It is well known that the transformation temperatures are strongly dependent on the Ni concentration rather than on Ti content [30], however it has been reported that near-equiatomic Ni-Ti compositions exhibit slightly higher transformation temperatures than Ti-rich and Ni-rich compositions [31-33]. Therefore, the formation of Ti-rich precipitates in the matrix caused a change in chemical composition toward a near equiatomic condition, thus making the films annealed at 600° fully martensitic at ambient temperature.

The XRD spectra in Fig. 4 show the microstructural evolution of the NiTi-base composition, annealed for 1 h at 500 and 600°C, when an increasing amount of Cu has been introduced in the films. For the films annealed at 500°C, peak intensity evolution clearly indicated an increase in M_s with increasing Cu content. This effect is due to the solubility of Ni in the B2 matrix decreasing with increasing Cu content [34], and a decreasing Ni content in the matrix is known to increase the transformation temperatures [35].

A peak associated with the $Ti(Ni, Cu)_2$ phase, which almost overlapped the martensitic peak for $2\theta \approx 41°$, appeared in the films with a high at.% Cu. The $Ti(Ni, Cu)_2$ phase, which usually nucleates along two perpendicular planes in the B2 matrix, is thought to have a tetragonal structure and a coherent interface with the matrix; however it is not considered to be a GP zone [16]. It has been reported that this tetragonal phase has a rather thin disk-like morphology which makes it hardly detectable by XRD analysis especially at relatively low annealing temperatures, such as 500°C. The reason for the appearance, albeit weak, of the $Ti(Ni, Cu)_2$ peaks in the XRD spectra may be attributed to the fact that with increasing Cu content the thin plate precipitates may become more densely dispersed in the matrix.

Fig. 4 also reports the XRD spectra of the films annealed for 1 h at 600°C, where a similar scenario to that of 500°C was observed except for the fact that the NiTi-base film annealed at 600°C was already fully martensitic at ambient temperature. Furthermore, the peaks associated with the $Ti(Ni, Cu)_2$ phase were more evident owing to the precipitate coarsening at this relatively high annealing temperature [16]. Although Cu addition further contributes to lowering the solubility of Ni in the B2 matrix with consequent increase of M_s, it has been reported that for a specific annealing temperature the increase of M_s with increasing Cu content saturates [10]. This suggests that when the Cu content increases above a certain limit, the chemical composition of the matrix and consequently the M_s is no longer strongly affected, therefore the Cu atoms may be segregated or present as precipitates in the matrix. This may be another reason for the appearance of more intense peaks related to $Ti(Ni, Cu)_2$ phase with

increasing Cu content (Fig. 4). We expect that with increasing Cu content and annealing temperature coarsened and more densely dispersed plate precipitates may appear in the grain interior, as well as excess atoms segregated at the grain boundaries.

It has been reported that Ni-Ti thin films with a Cu content higher than 10 at.% exhibit a single stage B2-B19 martensitic phase transition [30]. However, the XRD analysis performed in this study shown only the presence of B19' martensite for NiTiCu15 and NiTiCu18 annealed at 500 and 600°C, as also found by Gao et al. [36] for a $Ti_{44.6}Ni_{40.1}Cu_{15.3}$ thin film. The reason for this may be understood by considering the free energy of parent and native phases. It is known that the relative stability of the parent and native phases is governed by their chemical free energy, i.e. chemical composition, and by elastic free energy, i.e. lattice distortion [30]. As the B19 phase was not identified at both annealing temperatures, it can be suggested that the lattice distortions caused by the solid solution substitution of Ni by Cu atoms, did not affect the relative stability between parent and native phases. Similarly, the strain field generated around coherent or semi-coherent precipitates did not contribute significantly to change the elastic free energy of the system. Therefore, the other possible cause is the change in chemical composition. This means that the formation of (Ni, Cu)-rich precipitates as well as the segregation of excess atoms at the grain boundary may decrease the Cu content in the matrix below 10 at.%; as a consequence, B19' is energetically more favourable at ambient temperature.

2.2 Transmission electron microscopy

Fig. 5 shows the cross section of films doped with different Cu contents and annealed for 1 h at 500°C. It is clear that, regardless of the chemical composition, the grains exhibit a columnar morphology extending in most cases through the whole film thickness, whereas their lateral size, i.e. size parallel to the film surface, seems to be strongly affected by the composition. This dependence appears to be related to the Cu content for (Ni, Cu)-rich films

with an approximately constant Ni/Ti ratio. The NiTi-base film displayed grains with a lateral size larger than the film thickness, indicating that grain growth normal to the surface was limited by the substrate and the film surface, while lateral grain boundary migration took place promoting the formation of large grains. On the other hand, with increasing Cu content the lateral grain size gradually decreased reaching an average size of 150 nm for 17.5 at.% Cu. Fig. 5 provides some evidence concerning the mechanism of grain growth during the heat treatment. Beneath the surface of the films a competitive growth mechanism from top to bottom took place. It is well known that the boundary mobility can be very sensitive to the presence of solute; therefore the mechanism reported above may be related to the anisotropy in the surface chemical interaction of the solute atoms with the crystal faces [37]. Based on this, looking closely at the surfaces (Fig. 6), it seems that the grain # 1, whose growth was blocked, is surrounded by a more continuous network of segregated atoms, approximately 10 nm wide. Therefore, it is likely that the two adjacent grains (# 2 and # 3) grew, at least in the early stages, at the expense of grain # 1, where most of the solute atoms had segregated to its grain boundaries. EDX line scans across the grain boundaries showed a (Ni, Cu)-rich composition for the phase segregated at the interface. The presence of the high Ni concentration may be attributed to the lower solubility of Ni in the B2 matrix with increasing Cu content as previously reported. Therefore it is likely that for a sufficiently large Cu content, segregation of a (Ni, Cu)-rich phase at grain boundaries occurs during annealing, preceding grain coarsening. Comparing Fig. 5 (b) to (d), it is seen that the competitive growth mechanism was further encouraged causing the formation of smaller grains (~20 nm) beneath the film surface, especially for the film with high Cu content shown in Fig. 5 (d). Near the substrate lateral grain growth was governed by the competition in terms of impurity segregation between adjacent grains. Therefore, the grain refinement observed in Fig. 5 from (a) to (d) is very probably associated mainly with Cu and Ni segregation at the grain boundaries, which limits grain boundary mobility in direction parallel to the film surface. This

behaviour is in contrast to the case of the NiTi-base film where segregated phases were not observed at all. In Fig. 6 uniformly distributed bright streaks along two normal directions can be appreciated in grain # 3. XRD line scan across these bright streaks showed a (Ni, Cu)-rich Ni-Ti-Cu composition; thus, they are believed to be $Ti(Ni, Cu)_2$ precipitates (b.c.t. structure) [38]. Since the precipitates are very thin, they are hardly identified in the XRD spectra of films annealed at 500°C (particularly for low Cu content). Fig. 7 demonstrates that with increasing Cu content $Ti(Ni, Cu)_2$ plate precipitates decrease in size and become more densely distributed in the matrix.

The presence of the $Ti(Ni, Cu)_2$ phase and the (Ni, Cu)-rich phase segregated at the grain boundaries reinforces our hypothesis regarding the appearance of the B19' rather than B19 phase as a result of the change in chemical composition of the matrix.

3. Mechanical properties and microstructure

The mechanical response of the films has been probed by multiple-loading nanoindentation and the nano-hardness and Young's modulus have been measured. Fig. 8 shows the hardness as a function of the Cu content for two annealing temperatures; the vertical error bars may also include the effects of crystal anisotropy together with measurement errors.

The NiTi-base film exhibited almost the same hardness value for both annealing temperatures being very close to the value reported by Huang et al. for a martensitic Ti-48.3 at.% Ni thin film [39]. These results indicate that though the austenitic phase was still partially present in the film annealed for 1 h at 500°C (see figure 1), its nanoindentation response was mainly controlled by the martensitic reorientation process (detwinning) rather than by stress-induced martensitic transformation.

Regardless of annealing temperature the average hardness increased almost linearly with increasing Cu content. Such a response was caused by two factors, i.e. grain refinement and structural evolution in the grain interior with different annealing temperatures and Cu contents.

For the films annealed at 500°C the grain refinement as well as the constraining effect of the neighbouring grains became prominent with increasing Cu content, thus decreasing the deformation accommodated during the indentation process.

However, films annealed at 500°C exhibit a higher hardness compared to those annealed at 600°C. This is most likely related to the austenitic phase present in the Cu-doped Ni-Ti thin films annealed at the lower temperature. Nevertheless, the XRD spectra in figure 4 show that with a Cu content higher than 13 at.% the B19' phase became prominent in films annealed at 500°C; consequently the hardness tended to saturate with a further increase in Cu content. On the other hand, films annealed at 600°C were fully martensitic at ambient temperature and thus exhibited a lower hardness regardless of the Cu content.

The other reason, which may influence the hardness of the films, is the change in size and amount of the $Ti(Ni, Cu)_2$ plate precipitates in the grains, as well as the interface of these precipitates with the matrix, for different Cu contents and annealing temperatures. In particular, $Ti(Ni, Cu)_2$ plate precipitates are found to be more finely and densely dispersed in the grains with increasing Cu content (Fig. 7). While with increasing annealing temperature coarsened and lower densely distributed plate precipitates with a semi-coherent interface with the matrix are found [16].

This highlights the fact that with increasing both Cu content and annealing temperature the strengthening effect gained by precipitation hardening is degraded, consequently pronounced differences may be observed in mechanical properties, as is the case reported in figure 8. Such dissimilarity is not mainly associated with the difference of the relative amount of austenitic and martensitic phase present in the films annealed at different temperatures, as in that case the difference in hardness would decrease owing to the increasing amount of martensite with increasing Cu content in films annealed at 500°C, as confirmed by XRD analysis (Fig. 4). The difference in hardness becomes prominent in the range 13-20.4 at.% Cu, where it is the nature

of precipitates playing the major role in the response to stress rather than the relative amount of austenite (B2) and martensite (B19').

The elastic moduli for the films annealed at different temperatures and doped with Cu are reported in figure 9. These results suggest that the Young's modulus was not affected by the annealing temperatures, as the two curves are almost superimposed. For the NiTi-base films, the average elastic moduli reported in this study are close to those reported in other studies [39-40] for austenitic and martensitic Ni-Ti thin films. However, the error bars associated with the elastic moduli in figure 8 are almost superimposed, making it difficult to precisely distinguish the mechanisms involved during indentation.

Generally, it was also observed that doping with an amount of Cu below 4 at.% does not produce significant changes in mechanical properties while when the Cu content is increased above this threshold a clear increase in elastic modulus was observed and associated to both grain refinement and the constraining effect of neighbouring grains.

Zarnetta et al. [23] reported an average elastic modulus of approximately 115 GPa for a $Ti_{48}Ni_{48}Cu_{10}$ film, ~600 nm thick, annealed in vacuum for 1 h at 500°C. In this study a lower average value (~95 GPa) was determined for the NiTiCu12 film. This difference can be attributed to differences in grain sizes and morphologies between the films investigated here and those reported in the study mentioned above.

Conclusions

Ti-rich Ni-Ti and both Ti-rich and (Ni, Cu)-rich Ni-Ti-Cu thin films with an approximately constant Ni/Ti ratio and an increasing Cu content in the range 0 – 20.4 at.% were fabricated. Doping Ni-Ti thin films with Cu allowed the introduction of microstructural changes without significantly affecting the stability of the austenitic and martensitic phases. For Cu-doped Ni-Ti films, XRD analysis highlighted the presence of $Ti(Ni, Cu)_2$ plate precipitates in the matrix, which became more prominent with increasing annealing temperature and Cu content. TEM images showed, for Ni-Ti-Cu thin films, the segregation of a (Ni, Cu)-rich phase at grain

boundaries, which was the cause of the grain refinement induced by Cu addition. Grains exhibited a columnar structure extending through the whole films thickness, while their lateral size strongly depended on the Cu content. The lateral grain size decreased from an average of 3 μm for the NiTi-base film to 150 nm when this film was doped with 17.5 at.% Cu and annealed at 500°C. The effects of the microstructural changes, induced by doping with Cu, on the mechanical properties of Ni-Ti-Cu thin films were quantified by nanoindentation. Nano-hardness increased almost linearly with increasing Cu content in the range 4-13 at.% Cu, regardless of the annealing temperature owing to the grain refinement, though films annealed at 500°C exhibited higher hardness compared to those annealed at 600°C. This was due primarily to the austenitic phase still present in films annealed at 500°C. On the other hand for Cu content higher than 13 at.%, the structural evolution of $Ti(Ni, Cu)_2$ plate precipitates in the grains interior played a central role.

Young's modulus exhibited a similar dependence on Cu content; it increased almost linearly with decreasing grain size, i.e. increasing at.% Cu, irrespective of the annealing temperature.

As a conclusion alloying Ni-Ti compositions with a third element such as Cu, allows their mechanical properties to be modified by a certain extent, thus improving properties such as hardness and elastic modulus, which are among those factors that limit the use of NiTi-based thin films for tribological applications.

Acknowledgement

The research leading to these results has received funding from the European Union Seventh Framework Programme under a contract for an Integrated Infrastructure Initiative (Reference 312483-ESTEEM2).

This work was partially funded by the Ministry of Education of the Czech Republic (project MSM 6840770038.

References

1. F.F. Gong, H.M. Shen, Y.N. Wang, Mater. Lett., 15 (1995) 13-16.
2. S. Miyazaki, YQ Fu, WM Huang, Thin film shape memory alloys: fundamentals and device applications. Cambridge (UK), New York: Cambridge University Press, 2009.
3. Y. Fu, H. Du, S. Zhang, Surf. Coat. Technol., 167 (2003) 129-136.
4. W. Ni, YT Cheng, M. Lukitsch, A. M. Weiner, L. C. Lev, D. S. Grummon, Wear, 259 (2005) 842-848.
5. Y. Zhang, YT Cheng, D. S. Grummon, Surf. Coat. Technol., 202 (2007) 998-1002.
6. S. Miyazaki, A. Ishida, Mater. Sci. Eng., A 273-275 (1999) 166-133.
7. A. J. Muir Wood, S. Sanjabi, Y. Q. Fu, Z. H. Barber, T. W. Clyne, Surf. Coat. Technol., 202 (2008) 3115-3120.
8. T. Matsunaga, S. Kajiwara, K. Ogawa, T. Kikuchi, S. Miyazaki, Acta Mater. 49 (2001) 1921-1928.
9. A. Ishida, M. Sato, K. Ogawa, K. Yamada, Mater. Sci. Eng., A 438-440 (2006) 683-686.
10. A. Ishida and M. Sato, Philos. Mag., Vol. 87, No. 35, December 2007, 5523-5538.
11. A. Ishida and M. Sato, Philos.. Mag., Vol. 88, No. 16, June 2008, 2439-2448.
12. A. Ishida, M. Sato, Intermetallics, 19 (2011) 1878-1886.
13. A. Ishida, M. Sato, K. Ogawa, Mater. Sci. Eng., A 481-482 (2008) 91-94.
14. X. L. Meng, M. Sato, A. Ishida, Acta Mater., 56 (2008) 3394-3402.
15. A. Ishida, M. Sato, Intermetallics, 19 (2011) 900-907.
16. A. Ishida, M. Sato, K. Ogawa, Philos. Lett., Vol. 88, No. 16, June 2008, 2427-2438.
17. A. Ishida, M. Sato, K. Ogawa, Philos. Mag. Lett., Vol. 86, No. 1, January 2006, 13-20.
18. T. Matsunaga, S. Kajiwara, K. Ogawa, T. Kikuchi, S. Miyazaki, Acta Mater., 49 (2001) 1921-1928.
19. J. X. Zhang, M. Sato, A. Ishida, Acta Mater., 51 (2003) 3121-3130.

20. L. Zhang, C. Xie, J. Wu, J. Alloy Compd.., 427 (2007) 238-243.

21. A. Kumar, S. K. Sharma, S. Bysakh, S. V. Kamat, S. Mohan, J. Mater. Sci. Technol., 2010, 26(11), 961-966.

22. L. B. Tong, Y. H. Li, F. L. Meng, H. W. Tian, W. T. Zheng, Y. M. Wang, J. Alloy Compd., 494 (2010) 166-168.

23. R. Zarnetta, S. Kneip, Ch. Somsen, A. Ludwig, Mater. Sci. Eng., A 528 (2011) 6552-6557.

24. W. C. Oliver, G. M. Pharr, (1992) J. Mater. Res. 7 (6) 1564.

25. W. C. Oliver, G. M. Pharr, (2004) J. Mater. Res. 19 (1) 3.

26. Y. Q. Fu, S. Sanjabi, Z. H. Barber, T. W. Clyne, W. M. Huang et al., Appl. Phys. Lett. 89, 171922 (2006).

27. K Otsuka, C. M Wayman, Shape Memory Materials, Cambridge (UK), New York: Cambridge University Press, 1998.

28. A. Ishida, M. Sato, S. Miyazaki, Mater. Sci. Eng., A 273-275 (1999) 754-757.

29. P. Surbled, C. Clerc, B. Le Pioufle, M. Ataka, H. Fujita, Thin Solid Films, 401 (2001) 52-59.

30. K. Otzuka, X. Ren, Progress in Material Science, 50 (2005) 511-678.

31. J. P. Chu, Y. W. Lai, T. N. Lin, S. F. Wang, Mater. Sci. Eng., A 277 (2000) 11-17.

32. Y. Fu, H. Du, Surf. Coat. Technol., 153 (2002) 100-105.

33. S. Sanjabi, S. K. Sadrnezhaad, K. A. Yates, Z. H. Barber, Thin Solid Films, 491 (2005) 190-196.

34. A. Ishida, M. Sato, K. Ogawa, K. Yamada, Mater. Sci. Eng., A 438-440 (2006) 683-686.

35. S. Sanjabi, Z. H. Barber, Surf. Coat. Technol., 204 (2010) 1299-1304.

36. Z. Y. Gao, M. Sato, A. Ishida, J. Alloys Compd., 505 (2010) 81-85.

37. E. S. Machelin, An Introduction to Aspects of Thermodynamics and Kinetics Relevant to Materials Science, Elsevier, Linacre House, Jordan Hill, Oxford (UK), Third Edition (2007).

38. X. L. Meng, M. Sato, A. Ishida, Acta Mater., 57 (2009) 1525-1535.

39. X. Huang, J. Nohava, B. Zhang, A. G. Ramirez, Int. J. Smart Nano Mater., Vol 2, No. 1, March 2011, 39-49.

40. P. D. Tall, S. Ndiaye, A. C. Beye, Z. Zong, W. O. Soboyejo, H.-J. Lee, A. G. Ramirez, K. Rajan, Mater. Manuf. Processes, 22: 175-179, 2007.

Figure captions

Fig. 1 – Striations formed on the surface of the NiTi-base film after cooling from 600°C.

Fig. 2 – Cross-sectional SEM images of the Ni-Ti-base thin film: (a) as-deposited, (b) annealed at 500°C and (c) annealed at 600°C.

Fig. 3 – XRD spectra of the NiTi-base thin film in the as-deposited and annealed conditions (B2: austenite, B19': martensite).

Fig. 4 – XRD spectra of some of the investigated Ni-Ti-Cu thin films annealed for 1 h at 500 and 600°C.

Fig. 5 – Cross-sectional High Angle Annular Dark Field (HAADF) TEM images of (a) NiTi-base, (b) NiTiCu9, (c) NiTiCu15 and (d) NiTiCu18 annealed for 1 h at 500°C.

Fig. 6 – Cross-sectional HAADF TEM image of the NiTiCu9 film annealed for 1 h at 500°C.

Fig. 7 – Cross-sectional HAADF TEM images of the (a) NiTiCu13 and (b) NiTiCu15 thin films annealed for 1 h at 500°C. Smaller and more densely distributed $Ti(Ni, Cu)_2$ plate precipitates are observed for the NiTiCu15 film.

Fig. 8 – Indentation hardness as a function of Cu content and annealing temperature.

Fig. 9 – Young's modulus as a function of Cu content and annealing temperature, calculated using the elastic properties of the diamond Berkovich indenter (E=1141 GPa and ν=0.07) and assuming ν=0.3 for the films.

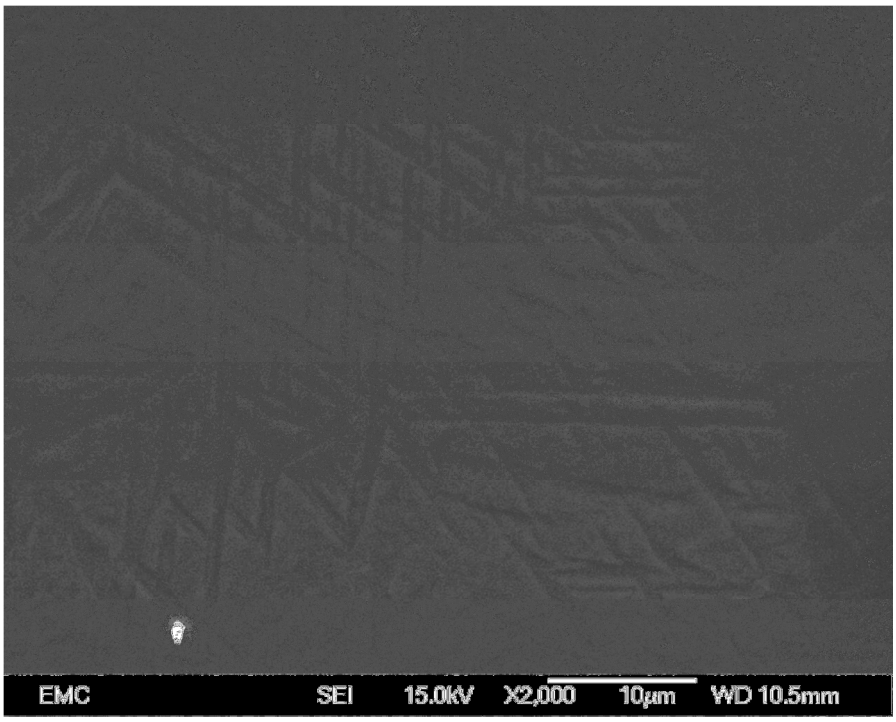

Fig. 1

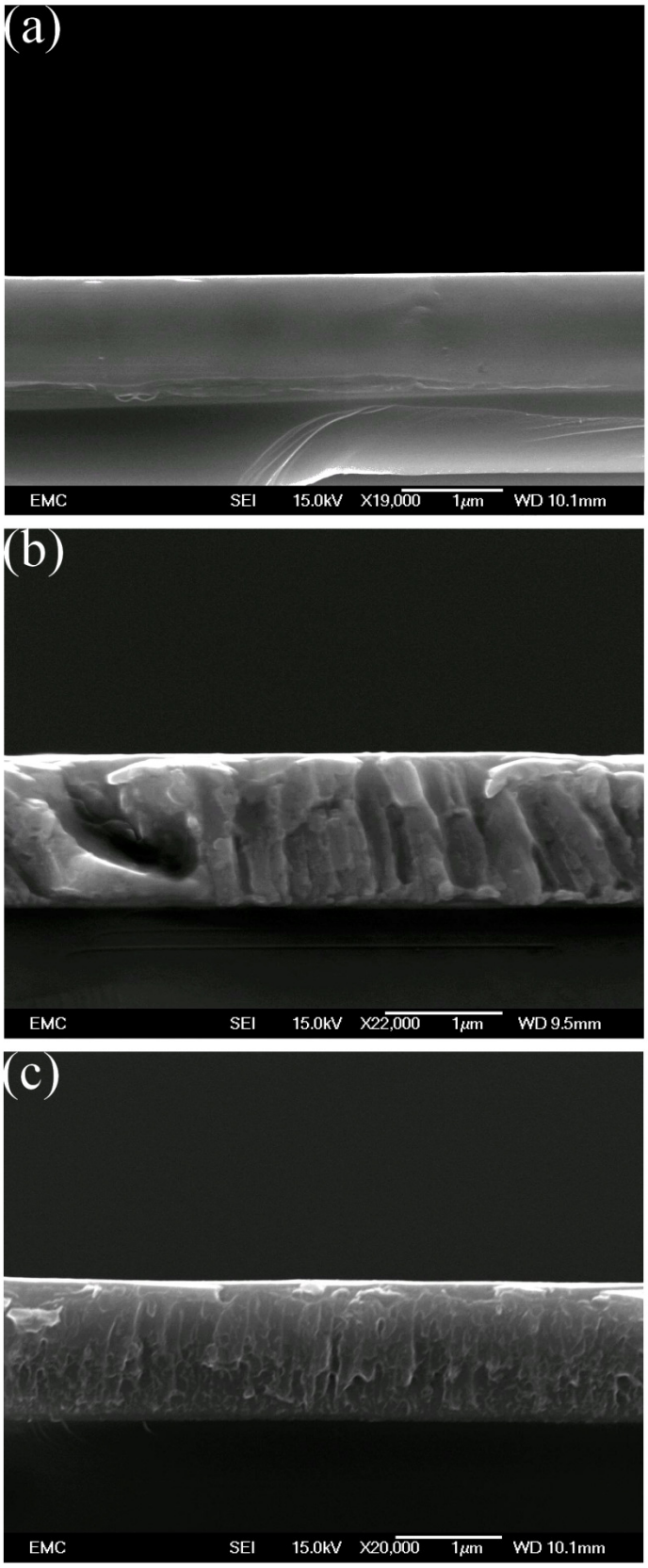
(a)
EMC SEI 15.0kV X19,000 1μm WD 10.1mm
(b)
EMC SEI 15.0kV X22,000 1μm WD 9.5mm
(c)
EMC SEI 15.0kV X20,000 1μm WD 10.1mm

Fig. 2

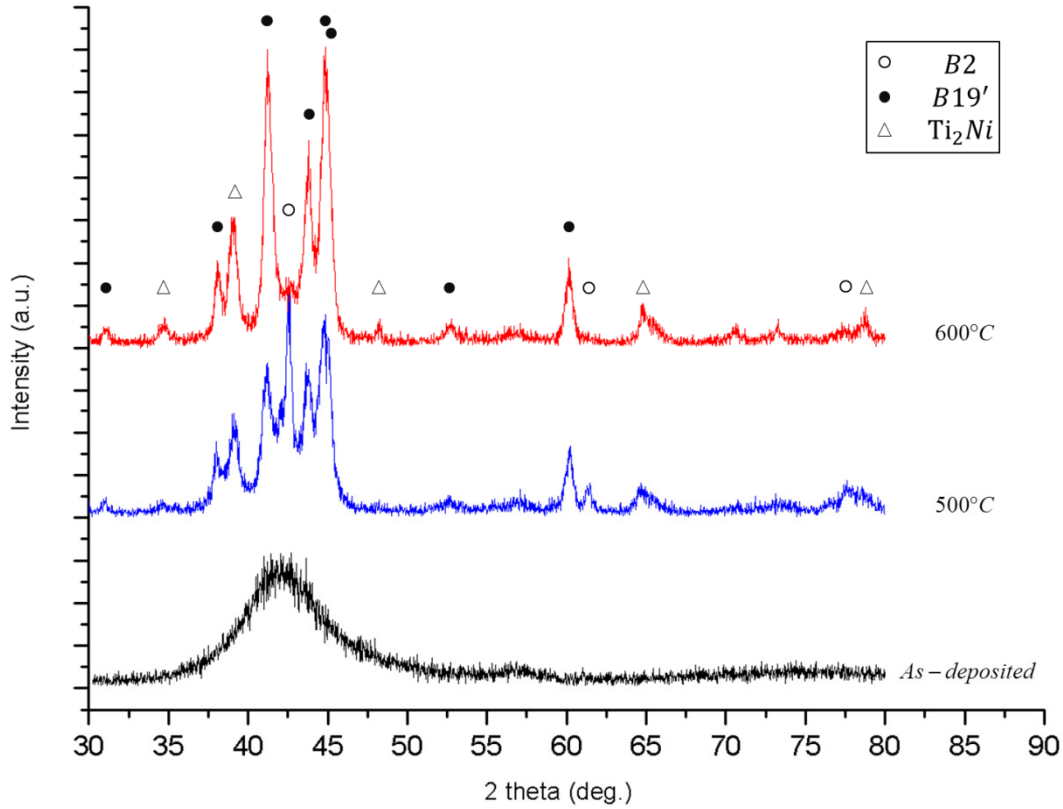
B2
B19′
Ti2Ni
600°C
500°C
As – deposited
Intensity (a.u.)
2 theta (deg.)
30 35 40 45 50 55 60 65 70 75 80 85 90

Fig. 3

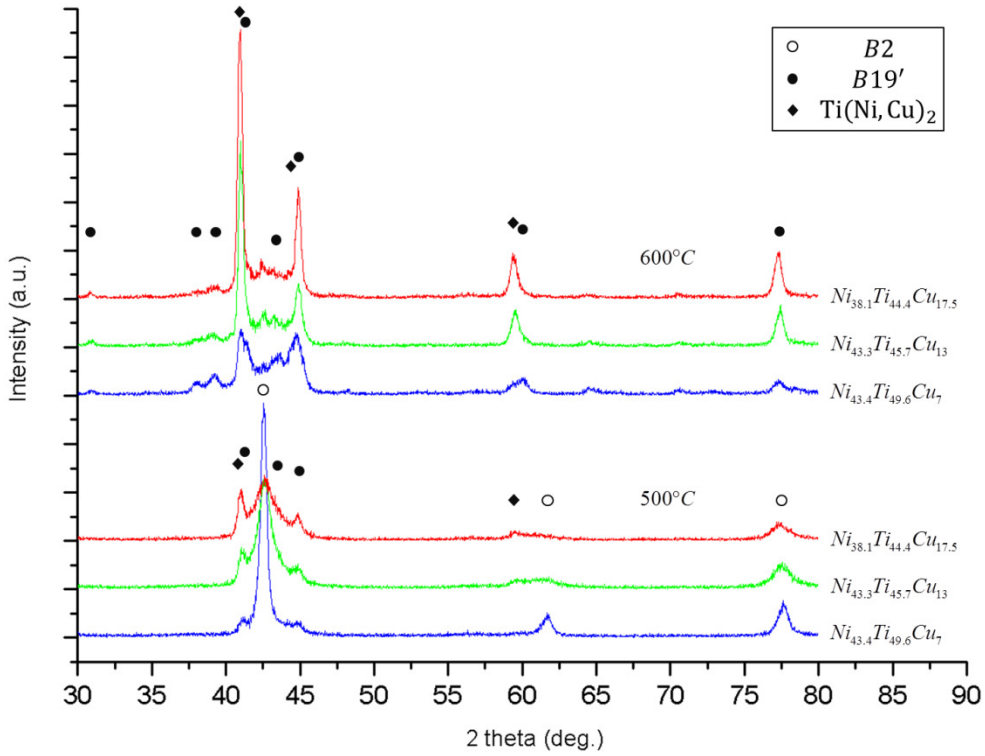
B2
B19′
Ti(Ni, Cu)2
600°C
Ni38.1Ti44.4Cu17.5
Ni43.3Ti45.7Cu13
Ni43.4Ti49.6Cu7
500°C
Ni38.1Ti44.4Cu17.5
Ni43.3Ti45.7Cu13
Ni43.4Ti49.6Cu7
Intensity (a.u.)
2 theta (deg.)
30 35 40 45 50 55 60 65 70 75 80 85 90

Fig. 4

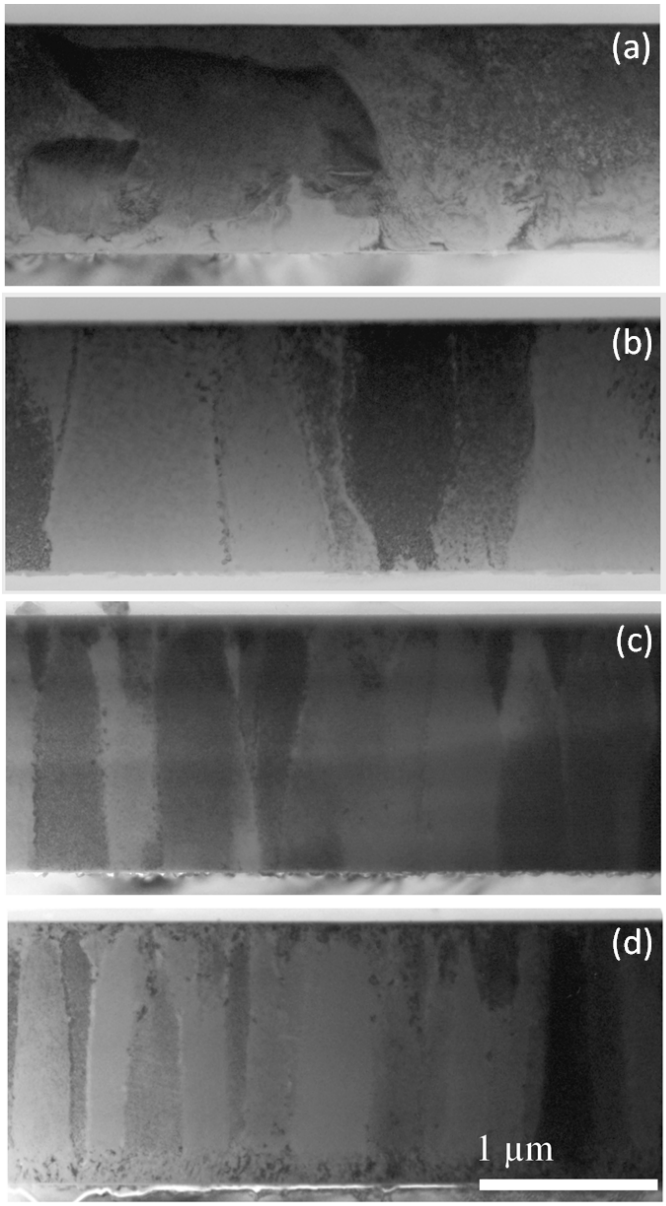

Fig. 5

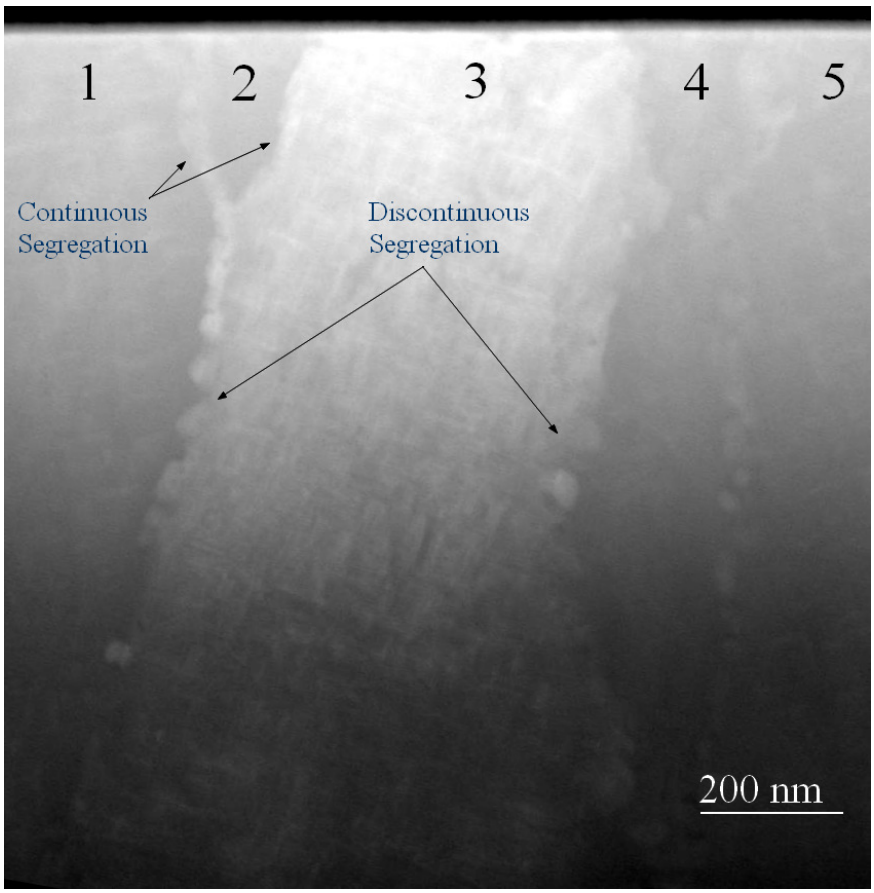
1
2
3
4
5
Continuous
Segregation
Discontinuous
Segregation
200 nm

Fig. 6

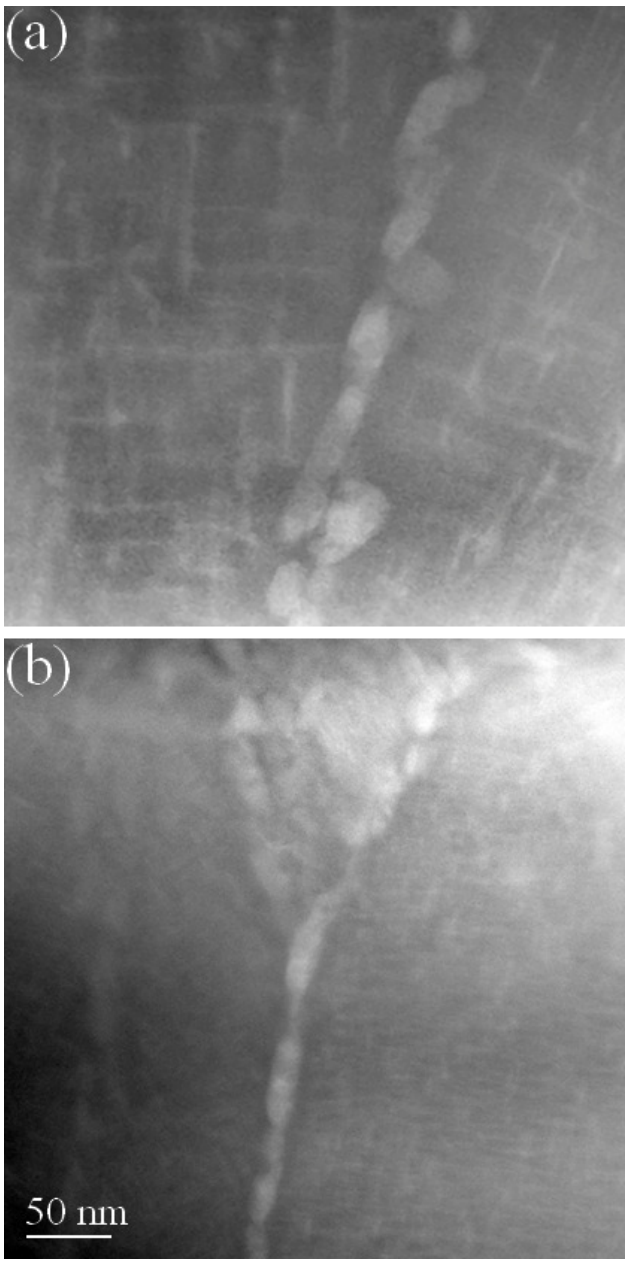

Fig. 7

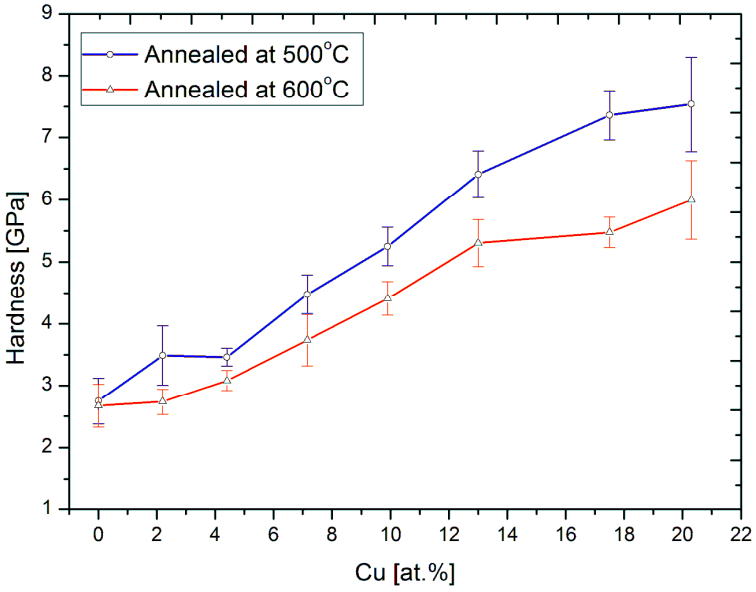
Annealed at 500°C
Annealed at 600°C
Hardness [GPa]
Cu [at.%]

Fig. 8

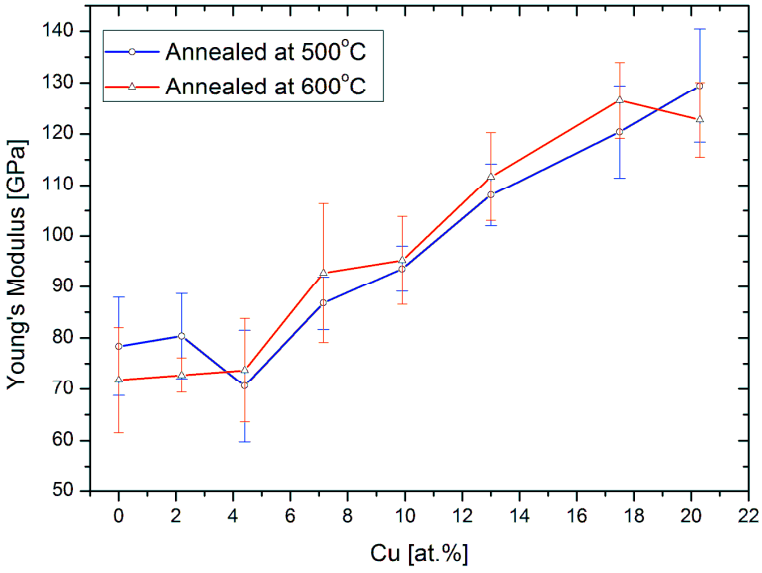
Annealed at 500°C
Annealed at 600°C
Young's Modulus [GPa]
Cu [at.%]

Fig.9